

# SUPERCONDUCTING PROPERTIES OF TITANIUM ALLOYS (Ti-64 AND Ti-6242) FOR CRITICAL CURRENT BARRELS

F. J. Ridgeon, M. J. Raine, D. P. Halliday, M. Lakrimi, A. Thomas and D. P. Hampshire

**Abstract**— We have measured the superconducting properties of the titanium alloy Ti-6Al-4V (Ti-64) as-supplied and following two of the heat treatment schedules used for the Nb<sub>3</sub>Sn strands in the ITER tokamak. The Ti-64 alloy is the standard choice in the superconducting community for the barrels used to make critical current ( $I_c$ ) measurements in high magnetic fields at cryogenic temperatures. Ti-64, which has a two-phase alpha + beta microstructure and contains vanadium (nb  $T_C(V) \sim 5.4$  K), is superconducting at 4.2 K in fields up to 3 T. We have also measured Ti-6Al-2Sn-4Zr-2Mo-0.2Si (Ti-6242), which is in the near alpha phase and contains tin (nb  $T_C(Sn) \sim 3.7$  K). The critical temperature of Ti-6242 is 2.38 K which is lower than the 5.12 K of Ti-64. Hence Ti-6242 is a better choice of barrel material for  $I_c$  measurements required at 4.2 K in low fields up to 3 T, because it remains in the normal state.

**Index Terms**— Titanium alloys, Critical current density, Upper critical field, Transition temperature, Metrology, Heat treatment,

## I. INTRODUCTION

THE conductors in the magnets of the ITER tokamak use Nb<sub>3</sub>Sn and Nb-Ti strands to produce the magnetic fields necessary to confine the plasma. To ensure uniform production quality, reference laboratories have measured the properties of the superconducting strands in high fields [1]: 12 T for Nb<sub>3</sub>Sn and 6.4 T for Nb-Ti at 4.22 K [2]. In standard critical current ( $I_c$ ) measurements at liquid helium temperatures, samples are usually measured on a Ti-6Al-4V wt % (Ti-64) ITER barrel [3]. Ti-64 is the workhorse of the titanium industry covering more than 50% of uses [4]. The excellent mechanical properties and good machinability of this material make it the material of choice for barrels [5]. It is a highly resistive material with low thermal conductivity which has a thermal contraction similar to Nb<sub>3</sub>Sn to minimize pre-straining of the strands [6]. The high electrical resistivity of Ti-64 at cryogenic temperatures is due to the high Ti content in solid solution [7].

However in 1970, Clark reported the electrical resistivity of many engineering alloys including the Ti-64 alloy and

reported that it exhibits a superconducting phase [8] at 4.2 K in magnetic fields of up to a few tesla [5]. Other reports followed: In 1992 Umezawa showed that the transition temperature ( $T_C$ ) of Ti-64 could vary between 4.35 and 6.3 K depending on oxygen concentration and heat treatment [9]. Divakar showed that  $T_C$  of Ti-64 could vary from 1.3 to 5.7 K [10], [11]. Barucci measured a  $T_C$  of about 4.38 K by a mutual inductance method [12]. We are interested in making  $I_c$  measurements of Nb-Ti and Nb<sub>3</sub>Sn on barrels across its entire range of magnetic field operation, including low fields, at 4.2 K [13]. Hence we have investigated the superconducting properties of the Ti-64 alloy, both as-supplied and heat-treated, as well as Ti-6Al-2Sn-4Zr-2Mo-0.2Si wt % (As Supplied), (Ti-6242 (AS)), which has similar electrical and material properties at room temperature to Ti-64 [7].

## II. MATERIALS AND MEASUREMENTS

### A. Material Properties

Ti-64 is categorised as an alpha + beta two-phase alloy with excellent strength and corrosion properties and good ductility. Ti-6242 is a near-alpha titanium alloy that is even stronger but less ductile. The origin of the superconducting properties of Ti-alloys is complex, but can be understood to some degree in terms of the Matthias rules [14] – the alloying both promotes the beta crystal structure and optimises the electron density of states [15]. Aluminium is included in both alloys. It stabilizes the alpha phase, which is probably not superconducting [4] and improves oxidation properties. The vanadium content of Ti-64 helps stabilise the beta phase which is probably the origin of the superconductivity [16] as does the molybdenum content in Ti-6242. The tin and zirconium in Ti-6242 are considered neutral in terms of stabilizing either the alpha or beta phase. Both titanium alloys have high electrical resistivity that does not change significantly from 10 K to room temperature. The thermal and mechanical properties of both alloys are given in Table I [7]. The thermal coefficient of linear expansion for Ti alloys is similar to the intermetallic superconductor Nb<sub>3</sub>Sn (i.e.  $7.6 \cdot 10^{-6} \text{ K}^{-1}$ ), but of course in practice, the thermal properties of a Ti alloy and a composite Nb<sub>3</sub>Sn strand, which includes softer materials such as copper that bring higher thermal contraction coefficients, are not perfectly matched [17]. We sort a barrel material with similar thermal and mechanical properties to Ti-64 but with a lower critical temperature. Although pure Ti and Al have values of  $T_C$  of only 0.4 K and 1.2 K, the vanadium in Ti-64 has the highest  $T_C$  (5.38 K) of the elements in the alloy and leads to  $T_C(\text{Ti-64}) \sim 5.12$  K. We chose to investigate the Ti-6242 alloy

Manuscript received September 06 2016; accepted DATE, 2016. Date of publication DATE, 2016; date of current version DATE, 2016. This work was supported by EPSRC Grant EP/L505419/1.

The authors F. J. Ridgeon, M. J. Raine, D. P. Halliday, and D. P. Hampshire are with Durham University, Superconductivity Group, Durham DH1 3LE (e-mail [f.j.ridgeon@durham.ac.uk](mailto:f.j.ridgeon@durham.ac.uk)).

The authors M. Lakrimi and A. Thomas are with Siemens plc: Healthcare Sector, MR Magnet Technology, Oxford, UK.

The data are available at Digital Object Identifier <http://dx.doi.org/10.15128/gh93gz498>

because it is in the near alpha phase and only contains elements with lower values of  $T_C$ . Ti-6242 contains tin - the highest  $T_C$  (3.772 K) of the elements in the alloy – which is orthorhombic in its pure state as well as Zr and Mo and as we report below, leads to  $T_C(\text{Ti-6242}) \sim 2.38$  K.

TABLE I HERE

### B. Heat treatments used for Ti-64

The heat treated Ti-64 samples measured in this work were cut from barrels used to react bronze route (Ti-64(BR) and internal tin (Ti-64(IT)) strands for  $I_C$  measurements for ITER. The heat treatment schedules for the Nb<sub>3</sub>Sn strands are outlined in Table II. The heat treatments were made using an argon atmosphere. Due to the low thermal conductivity of titanium alloys, the extraction of the small bars needed for the measurements was completed using low machine cutting speeds and large quantities of cutting fluid coolant. We expect the heating produced from extracting the titanium bars from the barrels is negligible.

TABLE II HERE

### C. Transport Measurements

Resistivity and the  $E$ - $J$  characteristics were measured as a function of temperature and magnetic field using a standard 4-terminal measurement. The samples were approximately 1 mm  $\times$  1 mm  $\times$  10 mm. Current and voltage leads were connected with silver paint such that the voltage taps were approximately 5 mm apart. The titanium bar samples were sequentially mounted into our 9 T Quantum Design, physical property measurement system (PPMS) on resistivity pucks and the in-built PPMS controls used to change temperature and field.

For the resistivity measurements, the internal PPMS circuitry was used. Uncertainties in the voltage gauge length, and hence absolute values of resistivity, derived from the cryogenic measurements on bars, were reduced to  $\sim 4\%$  by making an additional campaign of resistivity measurements at room temperature on longer 35 mm samples where the voltage tap separation was 20 mm. All the resistivity data in this paper are scaled by these more accurate room temperature resistivity data.

For the  $E$ - $J$  measurements on bars in the PPMS, external circuitry was used. The current was provided by a Keithley 220 programmable current source. A resistor was also added in series to the sample to ensure the nominal current programmed into the current source and the current derived from the voltage across the resistor were consistent through the measurements from 10 nA to 0.1 A. We measured the voltage across the sample using an amplifier of gain  $5 \times 10^4$  and a Keithley 2100 6½ digit multimeter. We also completed  $E$ - $J$  measurements on intact ITER barrels, modified to allow voltage taps to be connect to the Ti-alloy sections, and investigated the effect of field direction on the critical current density in these Ti-alloys using our vertical magnet system.

## III. RESULTS AND DISCUSSION

### A. Zero-field resistivity

The zero-field resistivity data for the titanium alloys are shown in Fig. 1. There is excellent agreement, to within 4 %, between our data, for the temperature dependence of the normal state resistivity of the as supplied Ti-64 alloy, and the data from Ekin and Clark [5], [8]. The two as-supplied alloys make a complete transition to zero resistivity as shown in Figs 1, 2 and 3.  $T_C(\text{Ti-6242}) \sim 2.38$  K is well below that of  $T_C(\text{Ti-64}) \sim 5.12$  K. The heat-treated sample Ti-64(BR) only shows partial transitions, where the resistivity drops by about 60 % as shown in Fig. 4. Table III summarizes  $T_C$ 's. We suggest this behavior is associated with some non-contiguous parts of this alloy becoming superconducting. The heat-treated sample Ti-64(IT) also shows (not shown here) similar partial transitions behavior.

FIG I HERE

### B. In-field resistivity

The titanium alloy samples were measured in-field to investigate upper critical fields: the superconducting critical temperature and upper critical field of the as-supplied Ti-64, are shown in Fig. 5 and are consistent with the literature. The heat treated Ti-64 alloys were also both measured in field. Fig. 3 shows the Ti-64(BR) data. We note that the Ti-64(IT) exhibits similar behavior. Although incomplete, the transitions remain relatively sharp and have a temperature dependence that we associate with a superconducting component in these alloys. We conclude that the superconducting path is not contiguous throughout the entire sample down to a base temperature of 2 K. It is known that temperatures of 620 °C are sufficient to change the microstructure of Ti-alloys consistent with these results [4]. The in-field transitions of the as-supplied Ti-6242(AS) alloy were also measured as shown in Fig. 3. They are very broad, consistent with multi-phase samples [18] containing materials with a range of compositions. The Ti-6242(AS) alloy also showed hysteretic resistive traces particularly in nominal zero field as shown in Fig.2. We attribute the hysteresis to trapped flux in these inhomogeneous samples. For each of the in-field traces in Fig. 3, the samples were first heated to above 3 K, to ensure the whole sample was driven normal.

FIG. 2 HERE

FIG. 3 HERE

FIG. 4 HERE

From the in-field resistivity measurements, a value for the onset of superconductivity was found ( $B_{c2}^*(T)$ ), for each alloy as shown in Fig. 5. The data have been fitted with using the well-known W-H-H empirical fit [19]. The characteristic superconducting and normal state parameters for the four alloys measured in this work are given in Table III.

FIG. 5 HERE

TABLE III HERE

### C. Critical current measurements

The critical current density ( $J_C$ ) measurements on bars of Ti-64(AS) and Ti-64(BR) at 4.2 K are shown in Figs. 6 and 7. The magnetic field was applied orthogonal to the direction of current flow. Ti-64(AS) shows a zero-resistivity base-line in contrast with and the Ti-64(BR) alloy which shows a resistive baseline from origin – both results are consistent with the data in Fig. 1. Critical current measurements on intact barrels were also completed for all four alloys at 4.2 K with the applied field parallel to the direction of current flow. Zero field data shown in Fig. 8 confirm that only the Ti-64(AS) alloy has a zero resistivity baseline from origin. It's  $J_C$  values in zero field were strongly hysteretic, which we often observe in samples measured in nominal zero field, and were about a factor of 3-4 higher than the data in Fig. 6 (42 mA mm<sup>-2</sup>). The increase in  $J_C$  is consistent with well-established Lorentz-free flux pinning considerations. The range of  $J_C$  values reported here are comparable to those of Goodrich [20], who found  $J_C$  values for barrels from > 680 mA mm<sup>-2</sup> for as-supplied material to 2 mA mm<sup>-2</sup> for annealed/oxidized barrels. It is important to note that these are not small values in the context of making high accuracy  $I_C$  measurements, since in zero field, the Ti-64 barrel can carry a supercurrent of > 112 A.

**FIG. 6 HERE**

**FIG. 7 HERE**

**FIG. 8 HERE**

### IV. CONCLUSION

We have measured the superconducting transition temperatures and upper critical fields of Ti-64 and Ti-6242 titanium alloys as well as the effect of two heat treatments on Ti-64. The critical temperature of Ti-64 is 5.14 K and that of Ti-6242 is 2.38 K. After the heat treatments, the standard Ti-64 no longer achieved the zero resistivity state but a partial transition in the resistivity was seen, which we attribute to isolated parts of the material remaining superconducting. We suggest that for high accuracy  $I_C$  measurements at 4.2 K in magnetic fields up to 3 T, the barrel should be made using Ti-6242 rather than Ti-64 because it is in its normal state.

### REFERENCES

- [1] M. C. Jewell, T. Boutboul, L. R. Oberli, F. Liu, Y. Wu, A. Vostner, *et al.*, "World-Wide Benchmarking of ITER Nb<sub>3</sub>Sn Strand Test Facilities," *IEEE Transactions on Applied Superconductivity*, vol. 20, pp. 1500-1503, 2010.
- [2] M. Sborchia, E. Barbero Soto, R. Batista, B. Bellesia, A. Bonito Oliva, E. Boter Rebollo, *et al.*, "Overview of ITER Magnet System and European Contribution," *IEEE/NPSS 24th Symposium on Fusion Engineering*, pp. 1-8, 2011.
- [3] IEC, "Superconductivity - Part 2: Critical current measurement - DC critical current of Nb<sub>3</sub>Sn composite superconductors," in *International Standard*, 1 ed: International Electrotechnical Commission, 1999, pp. IEC 61788-2.
- [4] C. Leyens and M. Peters, *Titanium and Titanium Alloys: Fundamentals and Applications*: Wiley VCH GmbH & Co. KGaA, 2003.
- [5] J. W. Ekin, *Experimental Techniques for Low-Temperature Measurements*. New York: Oxford University Press, 2007.
- [6] A. K. Ghosh, "Effect of Barrel Material on Critical Current Measurements of High- $J_C$  RRP Nb<sub>3</sub>Sn Wires," *IEEE Transactions on Applied Superconductivity*, vol. 21, pp. 2327-2330, Jun 2011.
- [7] R. Boyer, G. Welsch, and E. W. Collings, *Materials Properties Handbook: Titanium Alloys*: ASM International, 1993.
- [8] A. F. Clark, G. E. Childs, and G. H. Wallace, "Electrical resistivity of some engineering alloys at low temperatures," *Cryogenics*, vol. 10, pp. 295-&, 1970.
- [9] O. Umezawa and K. Ishikawa, "Electrical and thermal conductivities and magnetization of some austenitic steels, titanium and titanium alloys at cryogenic temperatures," *Cryogenics*, vol. 32, pp. 873-880, 1992.
- [10] U. Divakar, S. Henry, H. Kraus, and A. J. B. Tolhurst, "Measurement of the superconducting transition temperature of Dural and titanium 6Al-4V alloys," *Superconductor Science & Technology*, vol. 21, p. 3, Jun 2008.
- [11] U. Divakar, S. Henry, H. Kraus, and A. J. B. Tolhurst, "Corrigendum - Measurement of the superconducting transition temperature of Dural and titanium 6Al-4V alloys (vol 21, 065021, 2008)," *Superconductor Science & Technology*, vol. 23, p. 1, Dec 2010.
- [12] M. Barucci, L. Lolli, L. Risehari, and G. Ventura, "Measurement of thermal conductivity of the supports of CUORE cryostat," *Cryogenics*, vol. 48, pp. 166-168, Mar-Apr 2008.
- [13] S. A. Keys and D. P. Hampshire, "Characterisation of the transport critical current density for conductor applications," in *Handbook of Superconducting Materials*. vol. 2, D. Cardwell and D. Ginley, Eds., ed Bristol: IOP Publishing, 2003, pp. 1297-1322.
- [14] T. H. Geballe and J. K. Hulm, "Bernd Theodore Matthias," *National Academies Press*, 1996.
- [15] E. W. Collings, *A Sourcebook of Titanium Alloy Superconductivity*. New York: Plenum Press, 1983.
- [16] R. R. Hake, D. H. Leslie, and T. G. Berlincourt, "Electrical resistivity, Hall effect and superconductivity of some b.c.c. titanium-molybdenum alloys," *Journal of Physics and Chemistry of Solids*, vol. 20, pp. 177-186, 1961.
- [17] D. M. J. Taylor and D. P. Hampshire, "Properties of helical springs used to measure the axial strain dependence of the critical current density in superconducting wires," *Superconductor Science and Technology*, vol. 18, pp. 356-368, 2005.
- [18] R. R. Hake, D. H. Leslie, and T. G. Berlincourt, "Low-Temperature Resistivity Minima and Negative Magnetoresistivities in some Dilute Superconducting Ti Alloys," *Physical Review*, vol. 127, pp. 170-179, 1962.
- [19] M. S. Lubell, "Empirical scaling formulas for critical current and critical field for commercial NbTi," *IEEE Transactions on Magnetics*, vol. 19, pp. 754-757, 1983.
- [20] L. F. Goodrich, J. A. Wiejaczka, A. N. Srivastava, and T. C. Stauffer, "Superconductor Critical Current Standards for Fusion Applications," *NIST-Internal report (NISTIR)*, pp. 1-95, 1994.

TABLE I  
 THERMAL AND MECHANICAL PROPERTIES OF TITANIUM ALLOYS

	Ti-64 (AS)	Ti-6242 (AS)
Thermal Conductivity ( $W m^{-1} K^{-1}$ )	7.4	7
Thermal Coefficient of linear expansion ( $10^{-6} K^{-1}$ )	8.0	7.7
Specific Heat Capacity ( $kg^{-1} K^{-1}$ )	529	460
Young's Modulus: Tensile ( $10^{11} N m^{-2}$ )	1.10	1.14
Young's Modulus: Compressive ( $10^{11} N m^{-2}$ )	1.11	1.24

 TABLE II  
 HEAT TREATMENT SCHEDULES

Ti-64(BR) - Heat treatment schedule used for bronze route strand					
$T$ ( $^{\circ}C$ )	595	620	500		
Time (hours)	160	320	0		
Ti-64(IT) - Heat treatment schedule for internal tin strand					
$T$ ( $^{\circ}C$ )	210	340	450	575	650
Time (hours)	50	25	25	100	100

Heat treatment schedules used for the titanium alloys measured in this work. The barrels are first oxidised in air at  $300^{\circ}C$  in air for 5 h. Ti-64(BR) and Ti-64(IT) were then heat treated using the schedules that are used for the bronze route strands and internal tin strands (ITER Cycle B) in the ITER tokamak. A ramp rate of  $5^{\circ}C h^{-1}$  was used throughout. After the final heat treatment dwell, the temperature was rapidly decreased to room temperature by switching off the furnace.

 TABLE III  
 SUPERCONDUCTING AND NORMAL STATE PROPERTIES OF TITANIUM ALLOYS

	Ti-64 (AS)	Ti-64 (BR)	Ti-64 (IT)	Ti-6242 (AS)
$T_C$ (K)	5.12	5.50	4.52	2.38
$B_{c2}(0)$ (T)	8.45	9.03	6.74	3.55
$\rho(0, T, 273 K)$ ( $\mu\Omega m$ )	1.60	1.67	1.74	1.75
$\rho(0T, 10 K)$ ( $\mu\Omega m$ )	1.40	1.45	1.50	1.51

Transport measurements for the Titanium alloy Ti-64 (Ti-6Al-4V) and Ti-6242 (Ti-6Al-2Sn-4Zr-2Mo-0.2Si). The brackets (AS) denote 'as supplied'. Ti-64(BR) and Ti-64(IT) were heat treated using the schedules that are used for the bronze route strands and internal tin strands in the ITER tokamak as outlined in Table II.

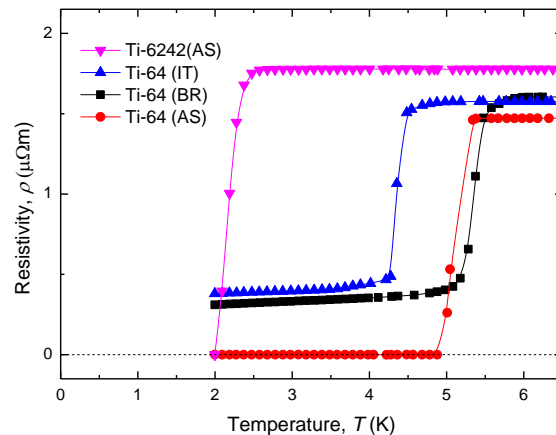


Fig. 1. The resistivity of titanium alloys Ti-64 (Ti-6Al-4V) and Ti-6242 (Ti-6Al-2Sn-4Zr-2Mo-0.2Si). The Ti-6242(AS) and Ti-64(AS) materials in the as-supplied state achieve zero resistivity. The Ti-64(BR) and Ti-64(IT) were heat treated using the schedules for bronze-route Nb<sub>3</sub>Sn and internal tin Nb<sub>3</sub>Sn strands respectively, as detailed in Table II. The heat-treated materials show partial resistivity transitions from their normal state resistivity to a lower resistivity value.

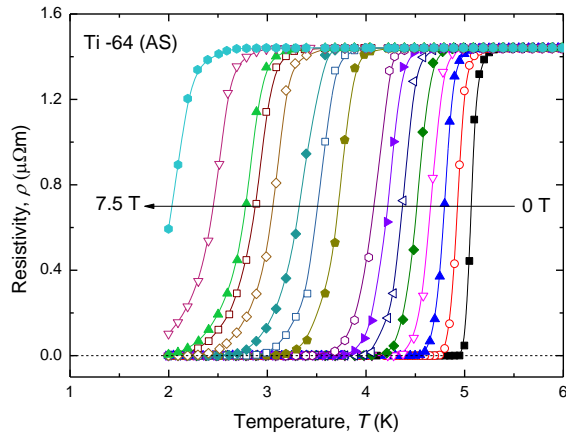


Fig. 2. The resistivity of as-supplied Ti-6Al-4V (Ti-64(AS)) as a function of temperature measured in magnetic fields from 0 T to 7.5 T in 0.5 T increments.

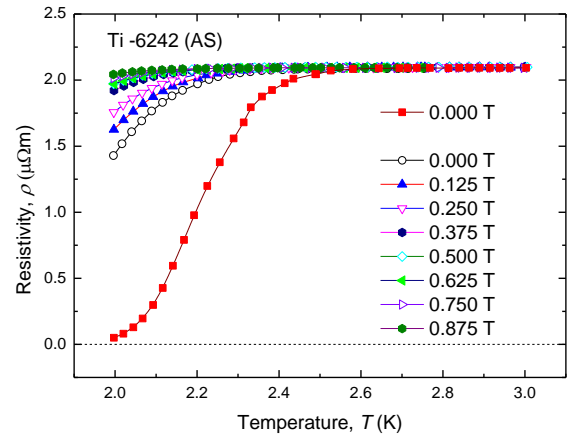


Fig. 3. The resistivity of as-supplied Ti-6Al-2Sn-4Zr-2Mo-0.2Si (Ti-6242(AS)) as a function of temperature measured in magnetic fields from 0 T to 0.875 T. The nominal 0 T data (1<sup>st</sup> run, red square) data were measured at the beginning of the experiment. The 0 T (2<sup>nd</sup> run, black unfilled circle) data were taken at the end of the experiment.

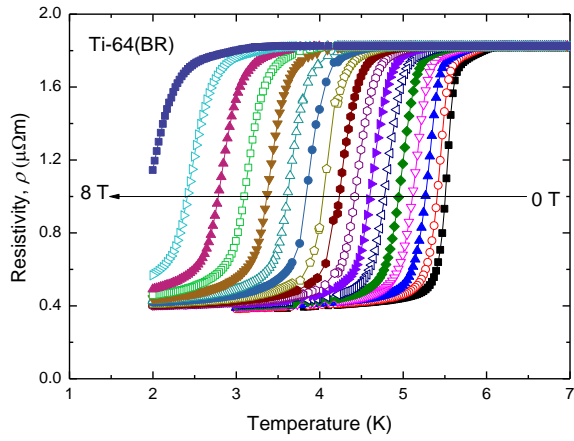


Fig. 4. The resistivity of Ti-6Al-4V heated treated (Ti-64(BR)) using the schedule used for bronze route Nb<sub>3</sub>Sn strands as given in table II, as a function of temperature measured in magnetic fields from 0 T to 8 T in 0.5 T increments. Note that at low temperatures the sample remains resistive.

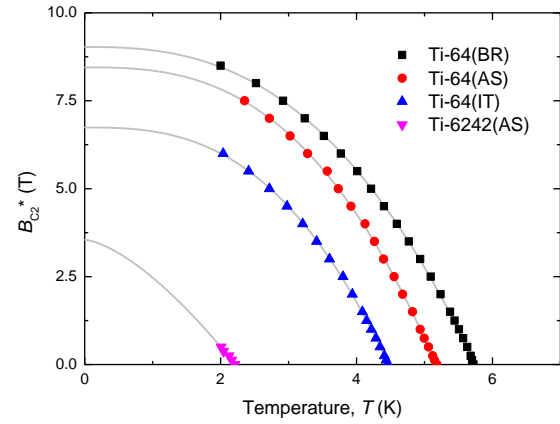


Fig. 5:  $B_{c2}^*(T)$  – the onset of superconductivity - for the as-supplied titanium alloys Ti-64(AS) (Ti-6Al-4V) and Ti-6242(AS) (Ti-6Al-2Sn-4Zr-2Mo-0.2Si) as a function of temperature. The onset was defined as 95% of the normal state resistance. The Ti-64(BR) and Ti-64(IT) were heat-treated using the schedules given in Table II. The solid line fits use the W-H-H equation [15].

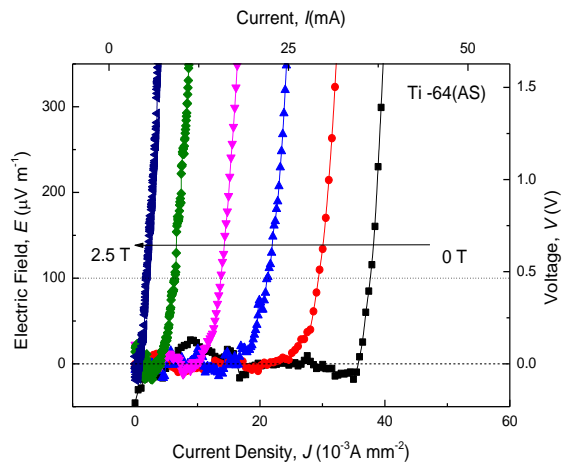


Fig. 6:  $E$ - $J$  characteristics at 4.2 K of as-supplied Ti-6Al-4V (Ti-64(AS)) between 0 T and 2.5 T in 0.5 T increments measured in increasing field.

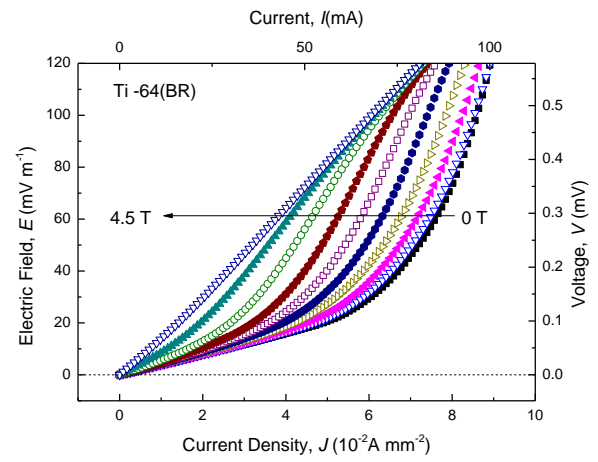


Fig. 7:  $E$ - $J$  characteristics at 4.2 K of Ti-6Al-4V heat treated using the schedule for bronze route  $Nb_3Sn$  given in Table II (Ti-64 (BR)). Measurements were made between 0 T and 4.5 T in 0.5 T increments. There is a resistive baseline from origin.

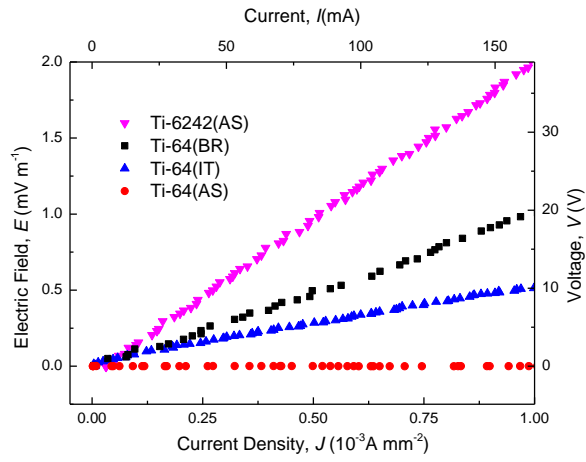


Fig. 8:  $E$ - $J$  characteristics at 4.2 K of titanium alloy barrels. Samples measured were Ti-64(AS) (as supplied Ti-6Al-4V); Ti-6242(AS) (as supplied Ti-6Al-2Sn-4Zr-2Mo-0.2Si) and Ti-64 that was heat treated using the internal tin (IT) and bronze route (BR) strand schedules given in Table II.